International Journal of Engineering & Technology, 7 (4.32) (2018) 25-29

International Journal of Engineering & Technology

Website: www.sciencepubco.com/index.php/IJET

Research paper

Novel Hsv Colour Space based Threshold Method for Vegetation Extraction and its Performance on Landsat TM Images

Abdelkrim Maarir[1]*, Abdelhalim Benyoucef[2], Belaid Bouikhalene[3]

[1]Computer Science Dept., Sultan Moulay Slimane University, Beni Mellal, Morocco
[2]Earth Sciences Dept., Sultan Moulay Slimane University, Beni Mellal, Morocco
[3]Mathematics and Computer Science Dept., Sultan Moulay Slimane University, Beni Mellal,
**Corresponding author E-mail: a.maarir@ieee.org*

Abstract

This paper deals with a novel proposed vegetation extraction method applied in multi spectral satellite images (Landsat TM). This proposed method essentially consists of three steps: image enhancement using histogram equalisation, image transformation to new colour model called HSV (Hue, Saturation, and Value) and thresholding application on Hue and Saturation components. For post-processing a hybrid filter median has been used to improve the results and remove isolated pixels. The proposed method is applied to three different scenes of Beni Mellal region in Morocco. The obtained results are compared with two other thresholding methods. Pixels identified as vegetation have an average sensitivity value of 95.88% and an accuracy value of 93.02%.

Keywords: *Vegetation extraction, HSV colour space, Thresholding, Hybrid filter, Satellite image.*

1. Introduction

Vegetation extraction is nowadays considered as one of the most important task in satellite images processing. It is most widely required in remote sensing in order to deals with land classification and land-use mapping [1], [2]. Vegetation is one of the main elements of change in the environment after atmosphere and hydrosphere. It has significant impact on climate and its long-term variations, as well as the availability of resources for humanity. The vegetation in all its forms provides a wide range of useful products to human life (food, energy, wood and oxygen).
Extraction and analysis of vegetation is done using images obtained from divers sources like satellites, aerial or hand-held platforms [3]. Satellite imagery is regularly used in many fields to study terrestrial biosphere over large areas as building localisation [4], [5] roads detection [6] and track seasonal and annual changes in vegetation cover. In the literature, several authors have presented different methods of vegetation mapping from satellite and aerial images. The most methods are based on Vegetation Indices (VI). VI is a simple measurement parameter of multispectral transformations, which is used to indicate earth surface vegetation cover and crops growth status in remote sensing [7]. It consists of converting luminance measured by a sensor into quantity and quality information. VI is widely used to identify and track plant dynamics and growth at a given time, as well as to estimate some biophysical and characteristic parameters of vegetation cover. There are several vegetation indices in use. They include the Difference Vegetation Index (DVI) which is equal to the difference between the near-infrared and red bands [8]. The Normalized Difference Vegetation Index or Tucker index [9] is the best known and most widely used. NDVI values lie between -1 and 1, where high NDVI values relate to the densest vegetation and low values corresponding to lack or vegetation low density. This vegetation index has been used in many previous studies [10], [11], for vegetation tracking [12], crop cover measuring [13] and vegetation change detection [14]. Decision trees method with spectral signature of vegetation was applied by Li [15] to get vegetation type classification. Vegetation and water surface features are extracted by using NDWI and NDVI features based on discrete wavelet transform and singular value decomposition in the approach proposed by Demirel and Anbarjafari [16]. Authors in [17], [18] used the NDVI to extract spectral signatures of different land cover types using a thresholding method. Inspired by those observations, in the present paper, we present our proposed method based on threshold method on HSV colour space for vegetation extraction from satellite images.

2. Methodology

In this section, we present study area material, data used and treatments applied. The diagram presented in Fig. 1 illustrates the flow of the proposed method.

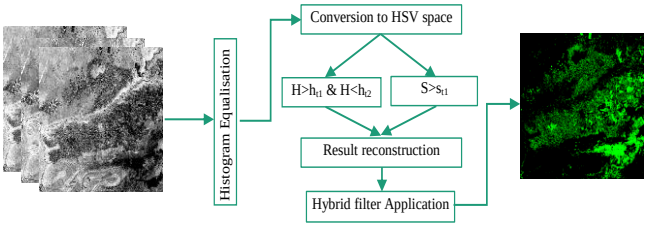

Fig. 2: Illustration on the proposed vegetation extraction approach.

2.1. Study area material

The location where the performance of the proposed method was tested is located in Beni Mellal - Khenifra region as shown in Fig.

Copyright © 2018 Authors. This is an open access article distributed under the Creative Commons Attribution License, which permits unrestricted use, distribution, and reproduction in any medium, provided the original work is properly cited.

2. It is situated in the middle of Morocco, covering an approximate area size of 46.47 km by 51.28 km, delimited between 32° 3' 40.22" N to 32° 35' 14.90" N and 6° 21' 21.14" W to 7° 2' 35.60" W.

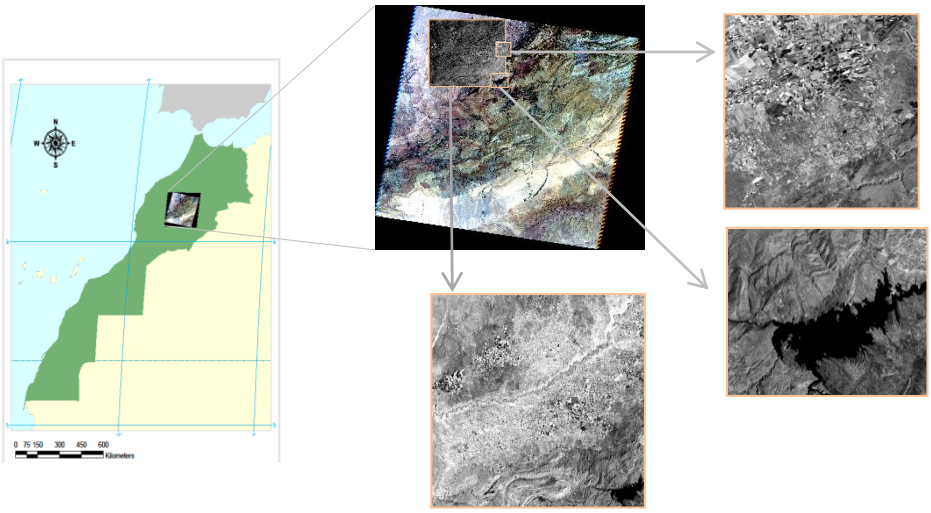

Fig. 2: Illustration on the proposed vegetation extraction approach.

The dominant vegetation in the study area consists of irrigated crops, olives and oak forest. Landsat orbit paths of the used images are 201 and 38 for rows. Required images for full study area are Landsat Thematic Mapper (TM) satellite imagery with 30 meters' spatial resolution, 2200 reflective samples and 1900 reflective lines and acquired on July 28, 2011.

2.2. Contrast enhancement by histogram equalisation

This enhancement is necessary for desert environments and when contrast is poor on an image.
Contrast enhancement was applied by using histogram equalisation technique in order to improve image appearance, adjust image intensity and enhance contrast. The proportion, as a fraction, of pixels associated with each digital number (DN) was calculated, and then the cumulative proportion was also determined. New DN value of each pixel is determined by the integer part of obtained result. Table 1 shows histogram equalisation values of the red band.

Table 1: Intensity distribution and histogram values for the red band

Input DN values	0	1	2	...	253	254	255
Number of pixels	251911	31150	0	...	0	0	78534
PA	0.0603	0.0075	0	…	0	0	0.0188
CP	0.0603	0.0678	0.0678	...	1	1	1
(L-1)*CP	15.3765	17.2890	17.2890	...	255	255	255
Output DN values	15	17	17	...	255	255	255

From the Table 1, PA is the probability appearance of each pixel intensity in the image matrix, CP is the cumulative probability and L is a constant that is equal to 256. This transformation is applied to the red band (TM3); it describes light distribution on the test image.

2.3. Vegetation extraction

After the contrast enhancement pre-processing steps, three TM bands were selected for use in a colour composite image. In order to obtain the best contrast of vegetation and to address the requirement of specific classification and thresholding guidelines in the target colour space, the band combination of TM 3, 4, 2 (RGB) was used. In this band combination the vegetation was highlighted in the colour green.
Vegetation extraction is performed in three steps:

- Converting initial image from initial colour space to the target one called Hue, Saturation and Value (HSV)[19].
- Histogram threshold application on Hue and Saturation components.
- Post-processing using a hybrid median filter.

2.4. HSV colour space

The identification of vegetation based on visible spectral space is seriously affected by the brightness of image, to solve this problem, a new colour space was chosen in which colours are not correlated with brightness. The HSV model has this property. Also known as HSB (Hue, Saturation, Brightness), the HSV model was proposed by Mundhenk [20]. It is a nonlinear transformation of the RGB colour model, and may be used in colour progressions. HSV defines a colour into three components and can be depicted using a hexagon in three dimensions as shown in Fig. 3.

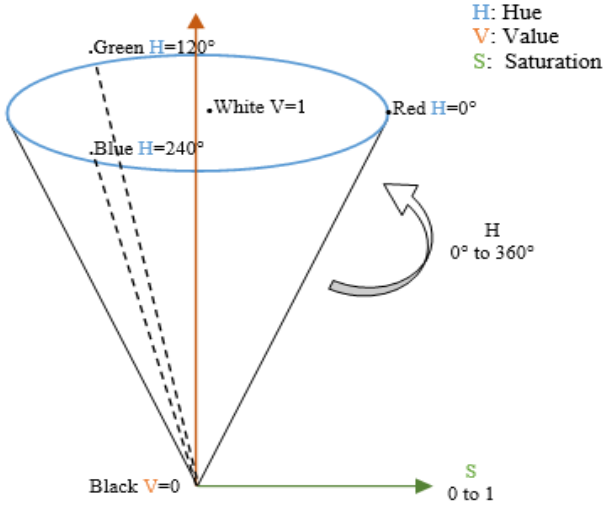

Fig. 3: Representation of the HSV colour space

From the illustration presented in the (Fig. 3), Hue represents colour type. It can be described in terms of an angle from 0 degrees to 360 degrees. This dimension has points normally called red from 0° to 60°, green from 120° to 180° blue from 240° to 300°, etc. The Hue model illustrates by the blue circle in the Fig. 3 above.
Saturation refers to the vibration of the colour and measures the departure of a hue from achromatic, it represents the intensity of a

specific colour type, and its value ranges from zero to one. The colour is grey when saturation value is zero and a primary colour in the other case.
Value simply refers to the brightness of the colour. It measures the departure of a hue from black. The range of values is between zero and one. For more detail see [20], [21]

2.5. Histogram threshold application on Hue and Saturation components

For vegetation extraction in colour space defined above, histograms of Hue and Saturation components are determined in Fig. 4, the identification of vegetation based on HSV colour space essentially comprises following 2 steps:
- H and S components thresholded
Hue and Saturation components will be segmented to identify pixels that represent vegetation in the image. By using a histogram thresholding, background pixels will be removed according to their hue and saturation values compared with the vegetation ones. The background suppression is defined according to the following (equations 1and 2).

$$H_{new} = \begin{cases} 1 & if\ H_{old} > h_{t1}\ and\ H_{old} < h_{t2} \\ 0 & otherwise \end{cases} \quad (1)$$

where, H_{old} are the digital values of the initial Hue component. h_{t1} and h_{t2} correspond to the lower and upper limits of the range which represents vegetation zone from histogram representation, as shown in the Fig. 4. H_{new} is a binary matrix. Pixels with zeros were identified as zones without vegetation and pixels with other values were identified as vegetation area.
The processed Saturation component is defined as follows:

$$S_{new} = \begin{cases} 1 & if\ S_{old} \in [s_{t1}, 1] \\ 0 & otherwise \end{cases} \quad (2)$$

here, s_{t1} is the smallest value of saturation component obtained from the histogram shown in next section. S_{new} pixels with ones' values were identified as vegetation zones.
– H_{new} and S_{new} components concatenated
In the processed Saturation component, pixels identified as vegetation contain other pixels which have values close to vegetation ones and represent water surface.
To eliminate the water pixels and keep the vegetation ones, a combined condition of Hue and Saturation value will set. H_{new} and S_{new} components are concatenated using the logical operator "&" as shown in equation 3. All preserved pixels correspond to the vegetation ones.

$$R_v = H_{new}\ \&\ S_{new} \quad (3)$$

As a result, a binary mask is obtained showing vegetation with value 1 and other land cover with 0.

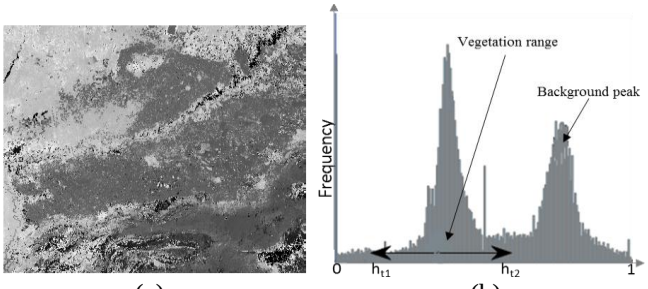

(a) (b)

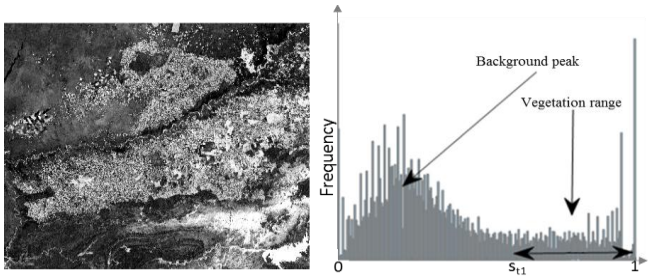

(c) (d)

Fig. 4: Threshold based on histogram: (a) (c) Processed Hue and Saturation components, (b) (d) Histogram display of image data.

2.6. Small objects removing

In order to eliminate isolated pixels, which are considered as noise, a hybrid median is used. This filter is based on a sliding kernel of n × n pixels moved over the initial image. Medians values of the vertical line pixels (V), horizontal line pixels (H) and central diagonal pixels (D) are calculated at the n × n window, the number of pixels in kernel is 5×5. By using median values of adjacent pixels on three directions, the final value (C) is equal to the median of the median values previously calculated (V), (H) and (D). This hybrid median filtering is better than the traditional median filter [21], since data from different directions zones are classified separately

3. Results and Discussion

The obtained results are presented to evaluate the performance of the proposed method. Vegetation extraction was done on multi spectral images and compared with other thresholding-based methods namely Heuristic thresholding and Otsu method [22]
The problem for vegetation extraction is to establish thresholding values (or thresholding interval). With too wide an interval, false positives are obtained, i.e. the thresholded image contains pixels that are not part of the objects of interest, usually it comes to noise, or structures of a different nature, which have a grayscale level close to desired object. With too close an interval, false negatives are obtained, i.e. some objects of interest do not appear, or only partially in the thresholded image. Therefore, we give below threshold values or thresholding intervals adopted for our method.
The Hue and Saturation histogram is shown in Fig. 4, which illustrates the application of the proposed method by following segmentation-based threshold. The first row shows Hue component. After several tests, we have deduced that vegetation zone is represented by the left part of the histogram which has a high frequency of light pixels and goes up strongly over the interval $[h_{t1}, h_{t2}]$, whereas in Saturation component (second row), the image is mainly composed of dark tones and light tones. The brightness difference between the background and the desired object (soil and vegetation) is very important, and so existence of other objects that have high contrast namely water. Pixels identified as vegetation are presented on the right side of the histogram that goes from s_{t1} to 1.
By analysing histograms of hue and saturation components, for Hue component there are two values: h_{t1} is set to 0.1 and h_{t2} is set to 0.5, for the Saturation component, the min threshold s_{t1} is set to 0.69. The obtained results are validated by the comparison with two other thresholding methods.
The proposed method was evaluated by using the NDVI index as reference images for validation. Three study scenes are chosen for that. With a statement of comparative accuracy with other methods, visually, the proposed method presents a better detection performance and that almost all the vegetation zones are detected reliably, as it can be seen in Fig. 5.

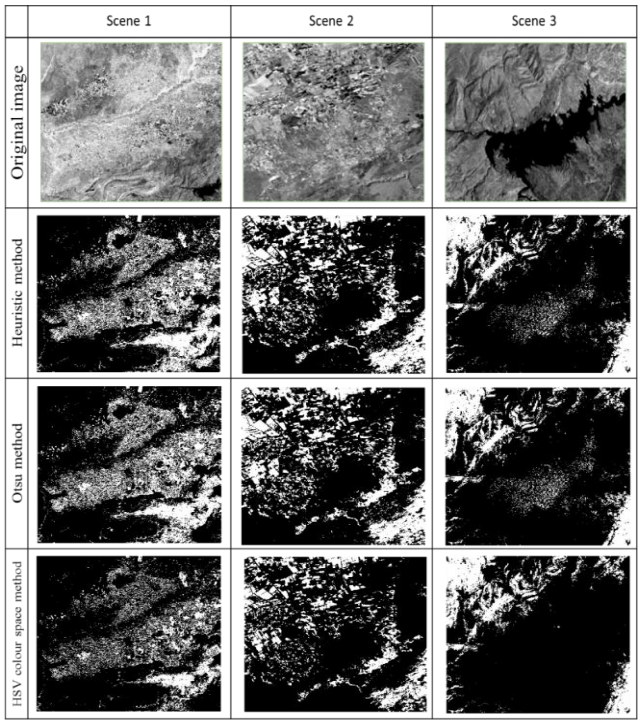

Fig. 5: Binary images display the comparison between the three applied methods: Heuristic thresholding, Otsu thresholding and the proposed method. Vegetation zones are represented by white pixels.

Performance validation

To assess classification accuracy, we used the following three measures described in equations (4), (5) and (6) in order to compare the results obtained, using the original image as reference. This technique was proposed by [23] and used to define the quality of vegetation extraction.

$$Sensitivity\ (SNS) = \frac{TP}{TP + FN} \tag{4}$$

$$Specificity\ (SPC) = \frac{TN}{TN + FP} \tag{5}$$

$$Accuracy\,(\mathrm{ACC}) = \frac{TP + TN}{TP + FN + TN + FP} \tag{6}$$

The measures described above depend on four major values: True Positive (TP), True Negative (TN), False Positive (FP) and False Negative (FN).

Here, TP are True pixels that represent vegetation and they are identified as vegetation (correct detection), TN are False pixels or no vegetation pixels are identified as no vegetation (correct detection), FP are True pixels that represent vegetation are identified as no vegetation (wrong detection) and FN are no vegetation pixels are identified as vegetation (wrong detection). Generally, TP, FN represent number of correct identification cases and FP, TN represent number of wrong identification case.

For a given classification, a performance measurement coefficient under 0.6 denotes that classification quality is low; a coefficient between 0.6 and 0.8 indicates a good classification quality and greater than 0.8 indicates a very good classification of one.

In order to prove that the proposed method can efficiently detect vegetation area, we compare our algorithm with Heuristic thresholding method and Otsu method by using training data.

To summarise our experiments, Table 2 lists the best performance results for every method in the same study area. In terms of SNS the proposed approach has a better rate in all scenes, for the first and second scene, it has also good rate of ACC, rates of ACC for proposed method, Otsu algorithm and Heuristic algorithm are 96.23%, 90.62% and 90.62% respectively. This evaluation demonstrates that our method is able to detect the vegetation zones. Generally, an average ACC of 93.02% and average SNS of 95.88 are obtained on three scenes of the study area.

Table 2. Results of the performance on SNS, SPC and ACC values for our method compared with other related methods. Important values are highlighted in bold.

Table 1: Results of the performance on SNS, SPC and ACC values for our method compared with other related methods. Important values are highlighted in bold.

Methods	Measures	Scene 1	Scene 2	Scene 3	Average
Otsu method	SNS	0.6713	0.9410	0.8902	0.8342
	SPC	**0.9952**	**0.9234**	0.9337	**0.9508**
	ACC	0.9062	**0.9276**	0.9274	0.9204
Heuristic method	SNC	0.6714	0.9426	0.8930	0.8357
	SPC	**0.9952**	0.9219	0.9332	0.9501
	ACC	0.9062	0.9268	0.9275	0.9202
HSV colour space method	SNS	**0.9508**	**0.9846**	**0.9409**	**0.9588**
	SPC	0.9646	0.8598	**0.9479**	0.9241
	ACC	**0.9623**	0.8813	**0.9469**	**0.9302**

4. Conclusion

This paper explains a novel method for vegetation extraction from multi spectral remote sensing images. Firstly, the Blue, Red and Near Infrared bands were pre-processed and converted to HSV colour space. Secondly, histogram equalisation method was applied on pre-processing images. Finally, different threshold values have been adopted for Hue and Saturation components in order to deal with vegetation areas and apply quantitative evaluation. Two threshold methods were used for comparison and validation. The evaluation was done in three different scenes in the study area and experimental results indicate that the proposed method can detect vegetation zones with a high accuracy and consistency. This paper is the starting point of further works. In the future, the proposed method will be developed in order to bring out vegetation change detection in multi temporal images.

References

[1] M. W. A. Halmy and P. E. Gessler, The application of ensemble techniques for land-cover classification in arid lands, Int. J. Remote Sens., vol. 36, no. 22, (2015),pp. 5613–5636.

[2] O. S. Ahmed et al., 'Hierarchical land cover and vegetation classification using multispectral data acquired from an unmanned aerial vehicle', Int. J. Remote Sens., vol. 38, no. 8–10, (2017), pp. 2037–2052.

[3] M.-C. Girard and C.-M. Girard, Traitement des données de télédétection - 2ème édition - Environnement et ressources naturelles, Dunod, 2010.

[4] M. Izadi and P. Saeedi, Automatic Building Detection in Aerial Images Using a Hierarchical Feature Based Image Segmentation, 20th International Conference on Pattern Recognition, (2010), pp. 472–475.

[5] A. Maarir, B. Bouikhalene, and Y. Chajri, Building Detection from Satellite Images based on Curvature Scale Space Method, Walailak J. Sci. Technol. WJST, vol. 14, no. 6, (2016), pp. 517–525.

[6] A. Maarir and B. Bouikhalene, Roads Detection from Satellite Images Based on Active Contour Model and Distance Transform, 13th International Conference on Computer Graphics, Imaging and Visualization (CGiV), (2016), pp. 94–98.

[7] A. Bannari, D. Morin, F. Bonn, and A. R. Huete, A review of vegetation indices, Remote Sens. Rev., vol. 13, no. 1–2, (1995), pp. 95–120.

[8] C. Bacour, F.-M. Bréon, and F. Maignan, Normalization of the directional effects in NOAA–AVHRR reflectance measurements for an improved monitoring of vegetation cycles, Remote Sens. Environ., vol. 102, no. 3, (2006), pp. 402–413.

[9] C. J. Tucker, Red and photographic infrared linear combinations for monitoring vegetation, Remote Sens. Environ., vol. 8, no. 2, (1979), pp. 127–150.

[10] J. Verbesselt, A. Zeileis, and M. Herold, Near real-time disturbance detection using satellite image time series, Remote Sens. Environ., vol. 123, (2012), pp. 98–108.

[11] B. DeVries, J. Verbesselt, L. Kooistra, and M. Herold, Robust monitoring of small-scale forest disturbances in a tropical montane

forest using Landsat time series, Remote Sens. Environ., vol. 161, (2015), pp. 107–121.
[12] Y. Yang, J. Zhu, C. Zhao, S. Liu, and X. Tong, The spatial continuity study of NDVI based on Kriging and BPNN algorithm, Math. Comput. Model., vol. 54, no. 3, (2011), pp. 1138–1144.
[13] D. M. El-Shikha, P. Waller, D. Hunsaker, T. Clarke, and E. Barnes, Ground-based remote sensing for assessing water and nitrogen status of broccoli, Agric. Water Manag., vol. 92, no. 3, (2007), pp. 183–193.
[14] G. M. Gandhi, S. Parthiban, N. Thummalu, and A. Christy, Ndvi: Vegetation Change Detection Using Remote Sensing and Gis – A Case Study of Vellore District, Procedia Comput. Sci., vol. 57, (2015), pp. 1199–1210.
[15] W. Li, J. Du, and B. Yi, Study on classification for vegetation spectral feature extraction method based on decision tree algorithm, International Conference on Image Analysis and Signal Processing, (2011), pp. 665–669.
[16] H. Demirel and G. Anbarjafari, Discrete Wavelet Transform-Based Satellite Image Resolution Enhancement, IEEE Trans. Geosci. Remote Sens., vol. 49, no. 6, (2011), pp. 1997–2004.
[17] A. K. Bhandari, A. Kumar, and G. K. Singh, Feature Extraction using Normalized Difference Vegetation Index (NDVI): A Case Study of Jabalpur City, Procedia Technol., vol. 6, (2012), pp. 612–621.
[18] A. K. Bhandari, A. Kumar, and G. K. Singh, Improved feature extraction scheme for satellite images using NDVI and NDWI technique based on DWT and SVD, Arab. J. Geosci., vol. 8, no. 9, (2015), pp. 6949–6966.
[19] A. R. Smith, Color Gamut Transform Pairs, in Proceedings of the 5th Annual Conference on Computer Graphics and Interactive Techniques, New York, NY, USA, (1978), pp. 12–19.
[20] T. N. Mundhenk, HSV color space, Encyclopedia of Microfluidics and Nanofluidics. Springer US, Boston, MA, (2007), pp. 793–793.
[21] J. S. Lim, Two-dimensional signal and image processing. 1990, http://adsabs.harvard.edu/abs/1990ph...book.....l.
[22] N. Otsu, A Threshold Selection Method from Gray-Level Histograms, IEEE Trans. Syst. Man Cybern., vol. 9, no. 1, (1979), pp. 62–66.
[23] D. M. Powers, Evaluation: from Precision, Recall and F-measure to ROC, Informedness, Markedness and Correlation, J. Mach. Learn. Technol., vol. 2, no. 1, (2011) , pp. 37–63.